KERNFORSCHUNGSZENTRUM

KARLSRUHE

August 1969

KFK 1029

Institut für Experimentelle Kernphysik

The Optimization of Helix Accelerators

H. Schopper

GESELLSCHAFT FUR KERNFORSCHUNG M. B. H.

KARLSRUHE

KERNFORSCHUNGSZENTRUM KARLSRUHE

August 1969 KFK 1029

Institut für Experimentelle Kernphysik

THE OPTIMIZATION OF HELIX ACCELERATORS

H. Schopper

Gesellschaft für Kernforschung mbH, Karlsruhe

Abstract

A systematic study of the optimization of a helix accelerator enables a better understanding of discrepancies in the literature and provides a new way of chosing the helix parameters. The losses in the helix are calculated in a more consistent manner from the sheath model. A high shunt impedance over a large range of particle momenta with comperatively few frequency jumps can be achieved. A helix accelerator seems to be useful for nucleon energies up to 200 MeV. A normal as well as superconducting helix is considered. The results are applicable to the acceleration of protons and heavy ions.

1. Introduction

The helix accelerator has been extensively studied some time ago [1-4]. The interest has recently been renewed since such an accelerator seems to be advantageous for the acceleration of heavy ions [5], but also for protons [6]. It seems that a helical structure is also specially suited for a superconducting accelerator. In all these cases, the use of low frequencies is favourable, although for different reasons. The main advantage of a helix lies in the fact that for a given wave length the diameter a is much smaller than for a cavity structure. Its main disadvantage stems from the decrease of the shunt impedance

with increasing particle momentum. Hence a helical accelerator was thought to be useful for proton energies up to 50 MeV only. However, the considerations presented here indicate that even energies of several hundred MeV could profitably be obtained with a helix.

In this paper only the unshielded helix will be treated, i.e. no outer conducting tube will be taken into account. It will be assumed that the radius of this tube is somewhat larger than $a + r_o$ where r_o is the characteristic radius of the field [+]. This condition can be realized in practice as will be shown later. In this case the losses in the shielding tube are small and do not effect the optimization procedure essentially.

Also the losses in the supports of the helix are neglected. If the accelerator is operated in the standing wave mode the supports can be placed at current nodes in which way the losses can be kept small. The correction factors due to the shield and the supports have been calculated [2,5] and can easily be applied to the expressions given here.

It will be assumed that the focussing elements do not restrict the diameter of the accelerating structure. This implies that most of the focussing elements have to be placed between the accelerating tanks. This can be done without destroying the stability of the particle motion [7]. For a superconducting helix intertankfocussing is imperative anyway.

2. General Relations

The helix has been treated theoretically by several authors [2,8] and equations for the fields have been derived as a function of the geometrical parameters of the helix. These calculations are

[+] Because of the exponential character of the Bessel functions K_o and K_1 the field has dropped to about 1/e at $r = r_o$.

performed for a sheath helix which consists of a cylindrical surface with infinite conductivity in a helical direction. It can be realized by one or several metal ribbons or tubes wound with radius a and pitch s (see fig. 1). In the ideal case there is no space between the metal ribbons. The number of strips or helices does not enter into the calculation and its choice leaves some freedome for technical considerations.

For an optimum design the shunt impedance

$$Z_s = \frac{E_z^2}{N_L} \tag{1}$$

which relates E_z the accelerating field and N_L the power loss per unit length, has to be made as high as possible. Z_s determines the essential part of the cost, i.e. the rf cost for a normal accelerator and the refrigeration cost for a superconducting accelerator.

The power loss is given by

$$N_L = \frac{1}{2} I^2 R \tag{2}$$

where I is the total current in the helix and R is the resistance of the helix per unit length. The current is related to the magnetic field by Maxwell's equation $\oint \vec{H}\, d\vec{s} = \vec{j}\, \vec{F}$. If it is assumed that the metal ribbon is very thin one obtaines for the integration path (1) in fig. 1

$$(H_z^i - H_z^a)\ s \cos\psi = I \cos\psi \tag{3a}$$

or for the integration path (2) in fig. 1

$$\left[(H_z^i - H_z^a) \cos\psi - (H_\varphi^i - H_\varphi^a) \sin\psi\right] \cdot 2\pi\, a \sin\psi = I \tag{3b}$$

Equ. (3a) and (3b) are equivalent, of course, but they will both be used. H^i and H^a are the magnetic fields at the inside and outside of the helix, respectively.

The field components which are of interest here are given by [8]

$$E_z^i = - \frac{I Z_o}{2\pi k_o r_o^2} K_o \left(\frac{a}{r_o}\right) I_o \left(\frac{r}{r_o}\right)$$

$$H_z^i = - \frac{I}{2\pi r_o} \operatorname{cotg}\psi \; K_1 \left(\frac{a}{r_o}\right) I_o \left(\frac{r}{r_o}\right) \qquad (4)$$

$$H_\varphi^i = - \frac{I}{2\pi r_o} K_o \left(\frac{a}{r_o}\right) I_1 \left(\frac{r}{r_o}\right)$$

with $k_o = 2\pi/\lambda_o$ where λ_o is the vacuum wave length.

The fields at the outside of the helix are obtained by exchanging the Bessel functions K and I.

The characteristic radius r_o is the inverse of the radial propagation constant $\gamma = 1/r_o$. It is related to the geometrical parameters of the helix by the dispersion relation which follows from the boundary conditions. It can be put into the form

$$(k_o/\gamma) \operatorname{cotg}\psi = \left[\frac{I_o(\gamma a) K_o(\gamma a)}{I_1(\gamma a) K_1(\gamma a)} \right]^{1/2} \qquad (5)$$

with $\operatorname{cotg}\psi = 2\pi a/s$

In order to accelerate particles the phase velocity v must be equal to the particle velocity. For v one finds

$$\beta_p = \frac{v}{c} = \left[1 + (\gamma/k_o)\right]^{-1/2} \tag{6}$$

or

$$(k_o/\gamma) = \beta_p \gamma_p = pc/E_o = \hat{p} \tag{7}$$

where $\gamma_p = (1 - \beta_p^2)^{-1/2}$ and p and E_o are particle momentum and rest energy, respectively.

With (7) the arguement of the Bessel functions can be written

$$x = \gamma a = \frac{k_o a}{pc/E_o} = \frac{2\pi\ a}{\lambda_o} \cdot \frac{1}{\hat{p}} \tag{8}$$

3. Power loss and shunt impedance

All the relations given so far are rigorous for a sheath helix with infinite conductivity. In order to compute the losses Johnson [2] considered a helix consisting of one cylindrical wire with diameter d. Since per unit length one has s turns the resistance per unit length is given by

$$R = R_s\ \phi\ \frac{2\pi a\ s}{\pi d\ \cos\varphi} \tag{9}$$

R_s is the surface resistance and ϕ is a form factor taking into account the uneven current distribution around the circumference of the wire. It was shown [2] that for practical purposes

$$\phi \cdot s/d \approx 4. \tag{10}$$

Combining equ. (1), (2), (3a), (4) and (9) one finds the shunt impedance

$$Z_s = \frac{Z_o^2}{a\, R_s}\, \frac{d}{\phi s}\, \cos\psi\, \frac{I_1(x)\, K_o(x)\, K_1(x)}{I_o(x)\,[I_o(x)\, K_1(x) + I_1(x)\, K_o(x)]^2} \qquad (11)$$

It is always assumed that the particles are close to the axis and hence $r = 0$ and $I_o(0) = 1$.

In contrast to the approximation (9) which has been introduced by Johnson and was used by other authors a somewhat different procedure will be adopted here. It seems more consistant with the sheath helix model to compute the power loss per unit length according to

$$N_L = \frac{1}{2}\, R_s\, |H|^2 \times \text{(surface area)} \qquad (12)$$

instead of equ. (2) where I is connected to the helix fields but R is derived for a wire. From (12), (4), (3b) and (1) one obtaines +)

$$Z_s = \frac{Z_o^2}{\pi a\, R_s} \cos^2\psi\, \frac{I_1(x)\, K_o(x)\, K_1(x)}{I_o(x)\,[I_o^2(x)\, K_1^2(x) + I_1^2(x)\, K_o^2(x)]} \qquad (13)$$

A comparison of (11) and (13) reveals that the two expressions are equivalent if the form factor is interpreted in the following way

$$\frac{d}{\phi s} = \frac{\cos\psi}{\pi} \cdot f \qquad \text{with } f = \frac{[I_o\, K_1 + I_1\, K_o]^2}{I_o^2 K_1^2 + I_1^2\, K_o^2} \qquad (14)$$

+) If the metal ribbons do not fill the whole width s a factor b/s should be added to the right side of equation (13) where b is the circumference of the ribbon.

If $\gamma \approx 1$ the approximation $(d/\phi s) \approx 1/4$ is quite reasonable since $\cos\psi$ is not much smaller than 1 for low particle velocities. Johnson's optimization lead to values of $x \approx 0{,}4$ and in this range $\gamma \approx 1{,}2$. Hence the approximation (10) seems to be justified.

However, as will be shown here a helix with $x \approx 1$ is more favourable and x up to 2 may occur in a practical accelerator. In this case the approximation (10) is no longer good since $\gamma = 1{,}55$ at $x = 1$ and $\gamma = 1{,}9$ at $x = 2$.
The consequences for the optimization will be discussed below.

4. Optimization of the shunt impedance

The shunt impedance Z_s depends on the particle momentum p, the rf wave length λ_o and the helix dimensions a and s (see fig. 1). To optimize Z_s for a given momentum p one has therefore three parameters to play with. This makes the optimization somewhat complicated and the two procedures published [2,5] thus far seem to disagree. In order to solve this discrepancy a systematic treatment will be given here. As a result a third way of chosing the parameters will be shown to be the most favourable one.

The 3 parameters λ_o, a and s are not independent. Since the phase velocity has to be matched to the particle velocity the dispersion relation must be fullfilled. With (7) we can put (5) into the form

$$\hat{p} \cdot 2\pi\, a = s\, (I_o K_o / I_1 K_1)^{1/2} \qquad (5a)$$

where $\hat{p} = pc/E_o$ is the normalized momentum.

Hence only 2 parameters can be chosen independently. As will be shown one more relation is obtained by the optimization procedure and consequently one is left with only one parameter to choose. This choice will be mainly determined by technical requirements.

It turns out that the optimization leads to different results depending on which parameter has been selected as independent. We shall discuss now all three possibilities and shall compare them afterwards considering the achievable shunt impedance, feasability and practicability.

4.1. Optimization for normal conductors

In this section we shall consider a helix at room temperature. Furthermore it will be assumed that the particle momenta are small ($pc/E_o \lesssim 0.2$) which implies that $\cos\psi \simeq 1$. Corrections which have to be applied for higher momenta will be considered in 4.3., but they do not change the whole procedure essentially.

For normal conductors the surface resistance is given by

$$R_s = \sqrt{\frac{\pi Z_o}{\lambda_o \sigma}} \tag{15}$$

where $Z_o = 137\ \Omega$ and σ is the conductivity. Since a helix could easily be silverplated the conductivity of silver $\sigma = 6\times10^7\,(\Omega m)^{-1}$ will be used in the following. If (15) is inserted into (11) or (13) one finds

$$Z_s = Z_o \sqrt{Z_o\ \lambda_o\ \sigma/\pi}\ \frac{d}{\phi s}\ \frac{\cos\psi}{a}\ (x^2\ I_1 K_o K_1 / I_o) \tag{16}$$

or

$$Z_s = Z_o \sqrt{Z_o\ \lambda_o\ \sigma/\pi}\ \frac{\cos^2\psi}{a\pi}\ \frac{I_1 K_o K_1}{I_o (I_o^2 K_1^2 + I_1^2 K_o^2)} \tag{17}$$

where the Bessel functions have the arguement x as defined by (8). These expressions are inconvenient since they contain the 3 parameters λ_o, $\underline{a}$ and x explicitely. Using (5a) and (8) one can eliminate one and write Z_s in such a way that it containes only x and one of $\underline{a}$, λ_o and s, respectively. The optimization is carried

out for x whereas λ_o, a or s are considered as free parameter. This leads to the following three cases:

Case I. free parameter: λ_o

$$Z_s = Z_o \sqrt{4\pi\, Z_o\, \sigma}\ \frac{\kappa}{\hat{p}\sqrt{\lambda_o}}\ \frac{1}{x}\ F \qquad (18)$$

with $\kappa = \frac{d}{\phi s}\cos\psi$; $\quad F = x^2\, I_1 K_o K_1 / I_o$

This is deduced from equ. (16). If equ. (17) is to be used instead one has to replace κ and F by κ' and F' respectively

$$\kappa' = (1/\pi)\cos^2\psi, \quad F' = (I_1 K_o K_1 / I_o)\ \left[I_o^{\,2} K_1^{\,2} + I_1^{\,2} K_o^{\,2}\right]^{-1}$$

This will be refered to as the "dashed version".

Case II. free parameter: a

$$Z_s = Z_o \sqrt{2\, Z_o \sigma}\ \frac{\kappa}{\sqrt{\hat{p}\cdot a}}\ \frac{1}{\sqrt{x}}\ F \qquad (19)$$

For κ and F the same applies as under case I

Case III. free parameter: s

$$Z_s = Z_o \sqrt{4\pi\, Z_o\, \sigma}\ \frac{\kappa}{\sqrt{s}}\ \frac{1}{\sqrt{x}}\ F \cdot \left(\frac{I_1 K_1}{I_o K_o}\right)^{1/4} \qquad (20)$$

Again κ and F are the same as for equ. (18). We shall discuss now these three cases.

Case I offers the most straight-forward procedure. If λ_o is chosen Z_s assumes the highest value if the function $\eta_o = x^{-1}F(x)$ or $\eta_o' = x^{-1} F'(x)$ has a maximum. These functions are displayed in fig. 2. The maxima are reached for $x_m \approx 0.4$ and $x_m \approx 0.55$, respectively. The accelerator can be designed in such a way that Z_s hast its maximum value for all momenta. This requires that $2\pi\ a/\lambda_o = x_m \cdot \hat{p}$. Hence with $\hat{p}$ and λ_o given $\underline{a}$ is uniquely determined and from (5a) also s can be computed. This is essentially the procedure suggested by Johnson [2] (without the dashed version, however).

If $\hat{p}$ increases $\underline{a}$ and s must also increase (see equ. (8) and (5a)). If $\underline{a}$ has become too large to be practical a jump to a lower λ_o is necessary. A disadvantage of case I is that Z_s decreases with $1/\hat{p}$. This can partly be compensated by the jump to a lower λ_o. An advantage of this case can be seen in the fact that $\underline{a}$ increases only proportional to $\hat{p}$ and therefore comparatively few frequency jumps are necessary.

To illustrate this behaviour numerical values are inserted into equ. (18) and one obtaines

$$Z_s = 9{,}6/(\hat{p}\sqrt{\lambda_o/m}) \quad M\Omega/m$$

or $$Z_s = 15{,}7\ (\hat{p}\sqrt{\lambda_o/m}) \quad M\Omega/m \quad \text{(dashed version)}$$

All the considerations for these two alternatives are quite similar except that the estimate of the losses as given in this paper (dashed version) leads to higher Z_s. Reality may lie in between the two equ. (18a). In order to be conservative only the lower value will be used in the following examples.

In fig. 3 the shunt impedance is displayed as function of $\hat{p}$ for three different wave lengths which were chosen arbitrarily. In the lower part $\underline{a}$ and s are shown as calculated with $x_m = 0.4$. This implies $r_o = a/x_m = (2{,}5a)$ and hence the outer shield of the helix has to have a rather large radius of about 4a. If a helix radius $a \approx 6$ cm is still considered to be tolerable a wave

length λ_o = 10 m could be used up to $\hat{p}$ = 0,1 (E = 5 MeV). A change to λ_o = 3 m brings a down to 2 cm whereas Z_s jumps to 90 MΩ/m (see arrows in fig. 3). The next change of λ_o would be necessary at about $\hat{p} \approx 0{,}3$ (E ≈ 40 MeV). In this way Z_s stays above 30 MΩ/m for proton energies up to 70 MeV and it is still 20 MΩ/m at 200 MeV. Such a helix accelerator compares favourably with an Alvarez structure which has a maximum Z_s of about 40 MΩ/m around $\hat{p}$ = 0,15 and with an iris structure with a typical $Z_s \approx$ 20 MΩ/m at high energies. With comparable shunt impedances the much simpler structure speaks in favour of the helix.

Of course, it should be noted that the shunt impedance for the helix applies to the travelling wave mode. For a standing wave operation it is smaller by a factor of two. Since the more pessimistic alternative of (18a) has been used practical values of Z_s for the standing wave mode should be close to the values given in fig. 3.

In case II the helix radius a is considered as independent parameter. This case has not been considered so far in the literature. However, it seems to be the most interesting one mainly because the helix diameter is dictated by the particle dynamics.

According to equ. (19) the function $\eta_1 = x^{-1/2}F(x)$ has to be optimized which gives $x_m \approx 0{,}6$ (or 0,8) (see fig. 4). However, since $x_m = (2\pi\, a/\lambda_o\hat{p})$ one would have to change λ_o continously if a and x_m are kept fixed and $\hat{p}$ increases. Since this is not practical one cannot stay at the maximum Z_s if $\hat{p}$ increases. If λ_o and a are kept constant x will vary. Inspection of fig. 2 shows that the optima are rather flat and therefore a change of x by a factor 2 can be tolerated without sacrificing too much. This implies however, that the optimization should be carried out for the variable $\hat{p}$ rather than (a/λ_o). For this purpose we write equ. (19).

$$Z_s = Z_o \sqrt{2\, Z_o \sigma}\ \frac{\kappa}{\sqrt{a}} \sqrt{\frac{\lambda_o}{a}}\ F = 80 \sqrt{\frac{cm}{a}} \sqrt{\frac{\lambda_o}{a}}\ F(x) \qquad (19a)$$

or for the dashed version $$Z_s = 107 \sqrt{\frac{cm}{a}} \sqrt{\frac{\lambda_o}{a}}\ F'(x)$$

From fig. 2 we gather that F(x) has the maximum at $x_m = 0{,}9$ ($x_m = 1{,}0$ for F'). Depending on the final energy of the accelerator one chooses now a momentum $\hat{p}_m$ for which Z_s should be maximum. Very crudely $\hat{p}_m$ will be half the design momentum. Then one has $(2\pi\ a/\lambda_o) = x_m \hat{p}_m$ and from this the ratio a/λ_o is fixed. The only parameter that is left is a. According to (19a) a should be made as small as possible in order to obtain a high shunt impedance. But the beam diameter will limit a to about 5 cm at injection and to 1 to 2 cm at high energies. The pitch s has to be changed such to fullfill the dispersion relation and s increases approximately proportional to $\hat{p}$ (see fig. 4).

If with increasing $\hat{p}$ the variable x has run approximately through the range 1.5 to 0.5 one gets too far away from the optimum of Z_s. Then it is advisable to choose a different $\hat{p}_m$ which results in a jump of a/λ_o and hence also of λ_o. From (19a) it follows that Z_s will decrease as $1/\sqrt{\hat{p}}$. This can partially be compensated by decreasing a.

For the purpose of illustration Z_s, λ_o/a and s/a are displayed in fig. 4 as functions of $\hat{p}$.

Since x can be allowed to change approximately by a factor of 2 $\hat{p}_m$ has also been chosen in steps of 2. As explained the maxima decrease proportional to $1/\sqrt{\hat{p}}$ for fixed a. An almost constant Z_s over the whole range of $\hat{p}$ can be obtained if a is twice as large for the first section of the accelerator which also meets the requirements of beam acceptance. It should further be noted that

$x \sim 1/\hat{p}$ and hence the maxima are wider than in case III where $x \sim \hat{p}^{-2}$.

In fig. 4 the dashed version of Z_s is also shown. If multiplied by 1/2 these curves agree almost with the undashed version. Hence the general remarks made for case I apply here also but the shunt impedance is almost twice as high.

A practical example corresponding to case II will be discussed in section 5.

In case III the pitch of the helix is considered as independent parameter. Klein [5] introduced this way of optimization since he considered the maximum field strength between helix turns (and hence the distance between turns) as the critical quantity.

Equ. (20) has the gratifying feature that Z_s does not depend on $\hat{p}$ and hence in principle Z_s could be kept constant for all $\hat{p}$. For this purpose the function $\eta_2 = x^{-1/2}\ F(x)\ (I_1K_1/I_oK_o)^{1/4}$ must be kept at its maximum at $x_m = 0{,}7$ (or $x_m = 0{,}85$ for the dashed version). With s and x_m given $\underline{a}$ and λ_o can be calculated using the dispersion relation. One finds that approximately $\underline{a} \sim 1/\hat{p}$ and $\lambda_o \sim \hat{p}^{-2}$. Since a continuous change of λ_o is not practical one has a similar situation as in case II. Instead of keeping x_m fixed it is more realistic to choose a fixed λ_o and allow x to vary over a certain range around x_m. If a certain momentum $\hat{p}_m$ is chosen for which Z_s should have a maximum the ratio λ_o/s follows from the dispersion relation (5a). With λ_o beeing fixed $\underline{a}$ has to be adjusted such that the dispersion relation is fullfilled for all $\hat{p}$.

A disadvantage of this procedure is that $x \sim a/\hat{p} \sim \hat{p}^{-2}$ with the consequence that the acceptable range of x-values is run through very quickly. This implies that more frequency jumps are necessary as in case II.

Inserting numbers into (20) one obtaines

$$Z_s = 500\ (s/cm)^{-1/2}\ \eta_2(x)\ M\Omega/m \qquad (20a)$$

or

$Z_s = 636\ (s/cm)^{-1/2}\ \eta'_2(x)\ M\Omega/m$ for the dashed version

For various values of $\hat{p}_m$ which were chosen arbitrarily Z_s, λ_o/s and a/s are shown in fig. 5. As one notices the height of the maxima is the same for different $\hat{p}_m$. However, a/s has to decrease rapidly +) and since the beam size puts a lower limit to a one will have to increase s which in turn reduces the shunt impedance. Hence in practice also case III yields a shunt impedance which decreases with increasing $\hat{p}$.

Comparison of the three cases

We have considered the cases in which alternatively λ_o, a or s is considered as independent parameter whereas the other two are determined by optimizing Z_s. In order to assess these three possibilities additional criteria have to be called upon.

From the experimental point of view the initial and final frequency should differ as little as possible since each frequency jump has the result that some rf waves are not filled with particles. This implies a reduced micro-duty cycle.

+) In practice it will be difficult to construct a helix with rapidly varying a. The curve for a shown in fig. 5 could be approximated by a step function [5]. In order to fullfill the dispersion relation s must also be varied. This results in a rather complicated structure.

The pitch of the helix s should not be much smaller than about 1 cm since the helix wire with cooling needs a diameter of about 0.5 cm leaving a gap of 0.5 cm for the maximum electric field. However, a helix with 2 or even more strands could be envisaged for which the total electric field would be distributed over several gaps.

Clearly the helix radius $\underline{a}$ is restricted to a certain range of values. Its smalles size is determined by the beam dynamics. A value of a 6 cm at injection and a 2 cm or even smaller at high energies seems to be acceptable. The radius of the outer helix shield is essentially determined by r_o. Since the characteristic radius $r_o = a/x$ is proportional to $\underline{a}$, the helix radius must not be too large.

With these criteria one obtaines the following comparison of the three cases:

Case I: The available rf power sources restrict the choice of λ_o very little. Hence there is no need to make λ_o the independent variable. $Z_s \sim 1/\hat{p}$ drops rather fast. On the other hand $\underline{a}$ increases only linearly with $\hat{p}$ and therefore only few frequency jumps will be necessary.

Case III: Inspecting the figures 3, 4 and 5 one notices that s is sufficiently large except at very low $\hat{p}$. Hence the need to choose s as independent variable will occure only in acceptional cases at extremely low injection energies. Case III is in certain respects the extrem of case I. Here the maximum values of Z_s are independent of $\hat{p}$ (see fig. 5) whereas in case I $Z_s \sim 1/\hat{p}$. On the other hand the maxima of fig. 5 are quite narrow which implies many frequency jumps.

Case II: This case is intermediate between I and III. $Z_s \sim 1/\sqrt{\hat{p}}$ drops less than in case I and the maxima of fig. 4 are wider than those of fig. 5. Hence fewer frequency jumps are necessary. Besides that it seems that the helix diameter is

indeed the critical size since it determines the beam acceptance. Indirectly the outside diameter of the structure is also proportional to $\underline{a}$ since $r_o = a/x_m$. As x_m is largest for case II a comparatively small shield diameter is required. The fact that $\underline{a}$ is constant for a whole accelerator section and that s changes almost linearly with $\hat{p}$ contribute to the simplicity of the design. In conclusion it seems that case II which has not been considered so far in the literature should be prefered to case I and III.

4.2. Optimization for a superconducting helix

Because of the small geometrical dimensions and the simplicity of the structure a helix accelerator seems to be of special interest for the application of superconductivity. If superfluid helium is used it seems that the cooling is particularly easy [7]. The small dimensions have the additional advantage that a helix fabricated of niobium can be easily baked out in available furnaces.

In the case of a superconductor the surface resistance can be written

$$R_s = R_o \left(\frac{0{,}3\ \mathrm{m}}{\lambda_o}\right)^{\alpha} \qquad (21)$$

with an arbitrary normalization at a wave length of 0.3 m.

R_o depends exponentially on the temperature and may assume values between 10^{-6} and 10^{-9} Ω. Our main interest concerns the frequency dependence. Experimentally the exponent $\alpha = 1.8$ was found [9] whereas theoretically a value close to 2 is expected. For simplicity we shall use the theoretical value in the following discussion.

If the expression for R_s is inserted into the equations (18), (19) and (20) one finds

$$\text{case I} \qquad Z_s = Z_N \frac{\lambda_o}{\hat{p}} \eta_o(x)$$

$$\text{case II} \qquad Z_s = Z_N/2\pi \cdot a\left(\frac{\lambda_o}{a}\right)^2 F(x) \tag{22}$$

$$\text{case III} \qquad Z_s = Z_N \, s\left(\frac{\lambda_o}{s}\right)^{3/2} \eta_2(x)$$

$$\text{with } Z_N = \frac{Z_o^2}{R_o} \frac{2\pi\kappa}{0,9}$$

Since the dependence on the variable x is exactly the same as for a helix at room temperature all the arguements given in section 4.1 are here also valid. The only difference is that Z_s depends now in a different way on the independent variable.

For <u>case I</u> Z_s is shown in fig. 6a. The longer wave lengths give larger values of Z_s and hence one should try to stay at the lowest possible frequency for as high values of $\hat{p}$ as possible. However, since the lower part of fig. 3 is here also valid one notices that <u>a</u> increases with $\hat{p}$ and hence a frequency jump will be necessary around $\hat{p} = 0.15$. Unfortunately such a jump to a higher frequency reduces Z_s in contrast to fig. 3 where it lead to an increase.

For <u>case II</u> Z_s is displayed in fig. 6b; as one notices the maximum value of Z_s is reduced by a factor of 4 if $\hat{p}_m$ is doubled. This is because $Z_s \sim (\lambda_o/a)^2$ and $2\pi\, a/\lambda_o = x_m \hat{p}_m$. Hence at first

glance one should think it advisable to position the maximum of Z_s just somewhat above the injection momentum and then use the same frequency all the way up to the highest momentum. Since $\underline{a}$ can be kept constant no difficulties should arise. However, if $\hat{p}$ is increased, x becomes smaller and hence the characteristic radius $r_o = a/x$ rises in proportion. Since the diameter of the helix shield is determined by r_o a frequency jump will be necessary if r_o has become too big. This frequency jump which might be required around $\hat{p} = 0.15$ is again accompanied by a sudden reduction of Z_s.

Fig. 6b shows clearly that $\hat{p}_m$ and hence the frequency should be chosen as low as possible and one might ask where the limit is. If $\hat{p}_m$ is made small s/a also becomes small (< 0.2). Too small values of s could be avoided to a certain extent by chosing $\underline{a}$ sufficiently large. A more serious limitation is again caused by r_o. If $\hat{p}_m$ is taken too low then r_o increases rapidly (see fig. 6b) and the radial dimension of the structure becomes too large.

In <u>case III</u> a change from a Z_s-curve belonging to a certain $\hat{p}_m$ to a curve corresponding to 2 $\hat{p}_m$ results in even a larger reduction of Z_s. Since $(\lambda_o/s) \sim \hat{p}_m^{-2}$ (see fig. 5) and $Z_s \sim (\lambda_o/s)^{3/2}$ according to equ. (22) one has $Z_s \sim \hat{p}_m^{-3}$. Hence a frequency jump leads to very small Z_s-values. On the other hand, without such a jump the helix radius becomes too small (see fig. 5). Therefore this case is of little interest for a superconducting helix.

In conclusion it may be stated that for a superconducting helical accelerator case II is also to be prefered mainly because of the same reasons as given in 4.1. In general a superconducting helix seems to be less adaquate to go to high energies. This is because the dimensions of the helix require a jump at a proton energy between 8 and 30 MeV and a second jump might become necessary at higher energies. However, although the shunt impedance determines the cost of the refrigerator its importance should not be overemphasized. Because of technological problems in preparing

the superconducting surfaces R_o can vary by factors of 5 or even more. Hence the small geometrical size and the simple construction may become the main arguements in favour of the helix. If some reduction of Z_s is accepted a helical accelerator could be interesting for energies up to several 100 MeV.

4.3. Optimization for large particle momenta

In section 4.1 and 4.2 it was assumed that cos is nearly constant. This approximation holds only for small particle momenta. It will be shown now that apart from a reduction of Z_s the general optimization procedure remains unchanged if the variation of $\cos\psi$ is taken into account.

From the dispersion relation (5) one immediately derives

$$\cos^2\psi = \frac{1}{1 + \hat{p}(I_1K_1/I_oK_o)} \tag{23}$$

$\cos^2\psi$ as a function of x is shown in fig. 7. As one notices $\cos^2\psi$ is close to unity for $\hat{p} < 0.1$ and has only a very weak dependence on x in the range $0.5 \leq x \leq 1$ where the optima have been found. Hence the values x_m at which Z_s has a maximum remain practically unchanged even if $\hat{p}$ is larger than 0.1. The only correction that has to be applied to the results given in 4.1 and 4.2 is that at high energies Z_s is somewhat reduced. Around 100 MeV this reduction amounts to about 20 %.

5. Examples

A complete optimization of an accelerator would have to include the cost of the accelerating structure and the building. This would be beyond the scope of this paper. The final choice of parameters will also depend rather critically on the final energy. In the case of a proton accelerator for several 100 MeV

most care will have to be given to the high energy part since it covers most of the length of the accelerator. For a heavy ion accelerator with an energy of about 10 MeV/nucleon the optimization at low $\hat{p}$ values is relevant.

The parameters given in the following tables should therefore only be considered as illustrative examples of the procedure outlined in the previous sections. All examples are based on case II.

In table 1 two examples for a helix at room temperatur are shown. In both cases an injection energy of 750 keV has been assumed. For the shunt impedance 3 values are given in the table corresponding to the initial maximum and final value for this particular section.

Example 1 shows a possible version of a 300 MeV proton lineac. The helix diameter is reduced by a factor of 2 goin from the first to the second section. This is suitable from the point of beam acceptance and provides that Z_s has about the same value for these two sections. If the injection energy could be increased to 3 MeV the first section could be omitted. At 35 MeV ($\hat{p}$ 0.28) it seems possible to jump immediately to the $\hat{p}_m = 0.4$ curve if $\underline{a}$ is reduced again. The shunt impedance obtained is still rather high. Alternatively $\underline{a}$ could be left the same (numbers in brackets). If the 3. section is omitted this example refers also to a 35 MeV accelerator.

Example 2 illustrates a possible 70 MeV accelerator. For the first section a = 4.3 cm was chosen again. If one jumps to the $\hat{p}_m = 0.2$ curve at 8 MeV ($\hat{p} = 0.13$) the final energy can be reached with 2 sections as shown in table 1. Alternatively an intermediate section for $\hat{p}_m = 0.1$ could be introduced. It seems, however, that the resulting increase of the mean shunt impedance does not justify the complication of two frequency changes.

In table 2 examples for a superconducting helix are presented. Again an injection energy of 750 keV was assumed. For a higher injection energy $\hat{p}_m$ should be increased correspondingly. Fig. 6b shows that as far as Z_s is concerned there is no reason to go to a higher frequency. The only limitation is given by the cross section of the structure. If it is assumed rather arbitrarily that a + r_o should not exceed 30 cm then a jump around $\hat{p}$ = 0.13 is necessary. Example 1 implies a transition to the $\hat{p}_m$ = 0.1 curve and a second transition to the $\hat{p}_m$ = 0.2 curve around 30 MeV. However, if some shunt impedance is sacrificed one can go directly to $\hat{p}_m$ = 0.2. This is shown in example 2. Example 3 corresponds to example 2 except that the helix diameter has been reduced. This gives a lower shunt impedance but a smaller structure. Of course, section 1 of example 2 could be combined with section 2 of example 3. This would result in a bigger frequency jump with a correspondingly lower duty cycle unless special provisious are foresee. Since no frequency jump is necessary above 30 MeV the accelerator could be terminated at any other energy below 200 MeV without changing the choice of the parameters. This might turn out as an advantage if such an accelerator is constructed in steps.

References

1. W. Walkinshaw and K. Wyllie, Math. Memo 57 (1948

2. K. Johnson, Chr. Michelsens, Inst.Beretn. 14 and 16 (1954) CERN-PS/KS 27 (1954)

3. G. Dome, R. Servrancks, L. Onde Electrique 37, 880 (1957)

4. W. Müller, J. Rembser, Nucl.Instr.Meth. 4, 202 (1959)

5. H. Klein, Die Beschleunigung schwerer Ionen mit der Wendelstruktur, unpublished report, Frankfurt, 1968

6. B.W. Montague, CERN, ISR-300/LIN/67-34 and 57 (1967)

7. C. Passow, International Conf. on Particle Accel., Jerevan, 1969

8. H. Kaden, A.E.Ü., 5, 399 and 534 (1951)

9. L. Szecsi, International Conf. on Particle Accel., Jerevan, 1969

Table 1

Helix at room temperatur

	Example 1	Example 2
1. section		
Energy (protons)	0.75 to 3 MeV	0.75 to 8 MeV
$\hat{p}_m$	0,05	0,05
a	4,3 cm	4,3 cm
λ_o	6 m (≙50 MHz)	6 m (50 MHz)
Z_s	46-53-46 MΩ/m	46-53-30 MΩ/m
s	0,9 to 1,5 cm	0,9 to 2,2 cm
2. section		
Energy	3 to 35 MeV	8 to 70 MeV
$\hat{p}_m$	0,1	0,2
a	2,15 cm	2,15 cm
λ_o	1,5 m (≙200 MHz)	75 (≙ 400 MHz)
Z_s	46-53-31 MΩ/m	30-38-28 MΩ/m
s	0,95 to 2,15 cm	1,6 to 3,5 cm
3. section		
Energy	35 to 300 MeV	
$\hat{p}_m$	0,4	
a	1,07 cm (2,15 cm)	
λ_o	19 cm ≙ 1,6 GHz (38 cm ≙ 800 MHz)	
Z_s	30-38-30 MΩ/m (21-27-21 MΩ/m)	
s	1,5 to 2,5 cm	

Table 2

Superconducting helix

	Example 1	Example 2	Example 3
1. section			
Energy (protons)	0,75 to 8 MeV	0,75 to 8 MeV	0,75 to 8 MeV
$\hat{p}_m$	0,05	0,05	0,05
a	7,2 cm	7,2 cm	3,6 cm
λ_o	10 m ≙ 30 MHz	10 m ≙ 30 MHz	5 m ≙ 60 MHz
r_o	7 to 22 cm	7 to 22 cm	3,5 to 11 cm
$2\pi\ Z_s/Z_N \times 10^{-4}$	1,3 - 1,6 -0,8	1,3 - 1,6 - 0,8	0,65 - 0,84 - 0,4
2. section			
Energy	8 to 30 MeV	8 to 200 MeV	8 to 200 MeV
$\hat{p}_m$	0,1	0,2	0,2
a	7,2 cm	7,2 cm	3,6 cm
λ_o	5 m ≙ 60 MHz	2,5 m ≙ 120 MHz	1,25 m ≙ 240 MHz
r_o	11 to 22 cm	5,4 to 22 cm	2,7 to 11 cm
$2\pi\ Z_s/Z_N \times 10^{-2}$	36 - 22	7,2 - 8,6 - 7,2	3,6 - 4,3 - 3,6
3. section			
Energy	30 to 200 MeV		
$\hat{p}_m$	0,2		
a	7,2 cm		
λ_o	2,5 m ≙ 120 MHz		
r_o	11 to 22 cm		
$2\pi\ Z_s/Z_N \times 10^{-2}$	8,3 - 7,2		

Captions to figures

Fig. 1 Dimensions of a sheath helix

Fig. 2 The functions η_o, η_1 and η_2 versus the variable $x = (2\pi\ a/\lambda_o\hat{p})$. The functions η_o', η_1' and η_2' are obtained by replacing F by F'.

Fig. 3 Case I (λ_o independent variable). Shunt impedance Z_s, helix radius a and pitch s as function of particle momentum $\hat{p} = pc/E_o$. Frequency jumps should approximately occur at the $\hat{p}$ values indicated by arrows.

Fig. 4 Case II (a independent variable). Shunt impedance $Z_s\sqrt{a}$, λ_o/a and s/a as function of $\hat{p}$. The two sets of curves for Z_s correspond to the two equations (19a). Dashed curves belong to the "dashed version", they are reduced by 1/2. The arrows correspond to the frequency jumps between the sections of the examples of table 1.

Fig. 5 Case III (s independent variable). Shunt impedance $Z_s\ \sqrt{s}$, λ_o/s and a/s as function of $\hat{p}$. The arrows indicate possible transitions from one section to the next.

Fig. 6 The normalized shunt impedance Z_s for a superconducting helix accelerator.

Fig. 6a) refers to case I. Three arbitrary wave lengths are chosen as parameters.

Fig. 6b) refers to case II. The ratio r_o/a is also shown. The arrow indicates a possible transition.

Fig. 7 The function $\cos^2\psi$ as given by equ. (23) versus $x = (2\pi\ a/\lambda_o\hat{p})$ with $\hat{p}$ as parameter.

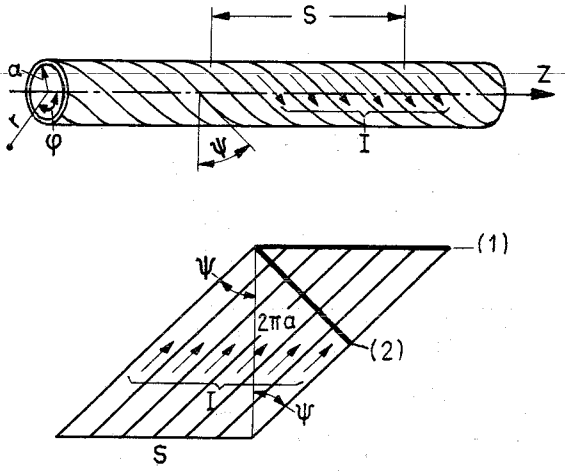

Fig. 1

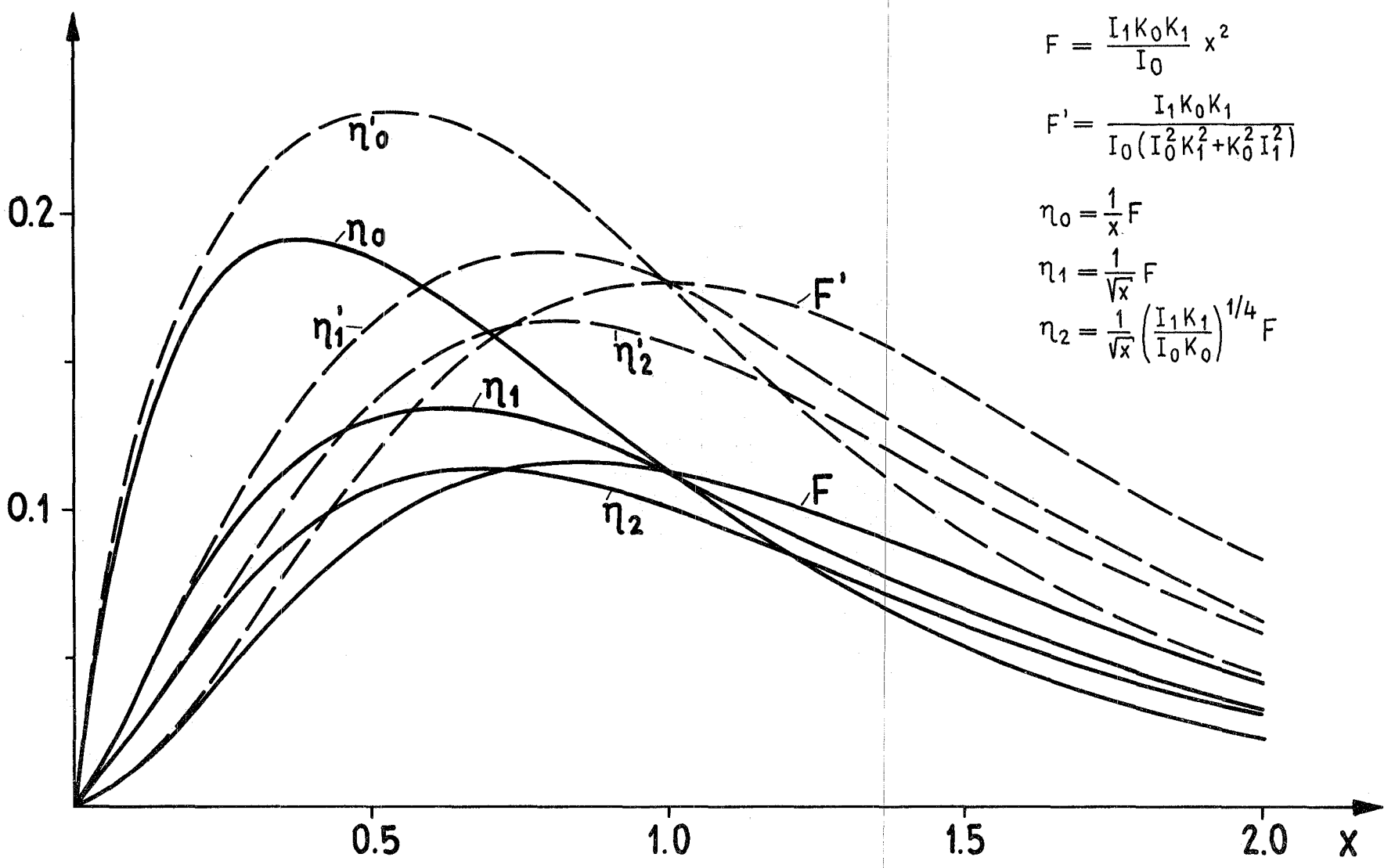
$F = \frac{I_1 K_0 K_1}{I_0} x^2$
$F' = \frac{I_1 K_0 K_1}{I_0 (I_0^2 K_1^2 + K_0^2 I_1^2)}$
$\eta_0 = \frac{1}{x} F$
$\eta_1 = \frac{1}{\sqrt{x}} F$
$\eta_2 = \frac{1}{\sqrt{x}} \left(\frac{I_1 K_1}{I_0 K_0}\right)^{1/4} F$
η'_0
η_0
η'_1
η'_2
η_1
η_2
F'
F
0.2
0.1
0.5
1.0
1.5
2.0
x

Fig. 2

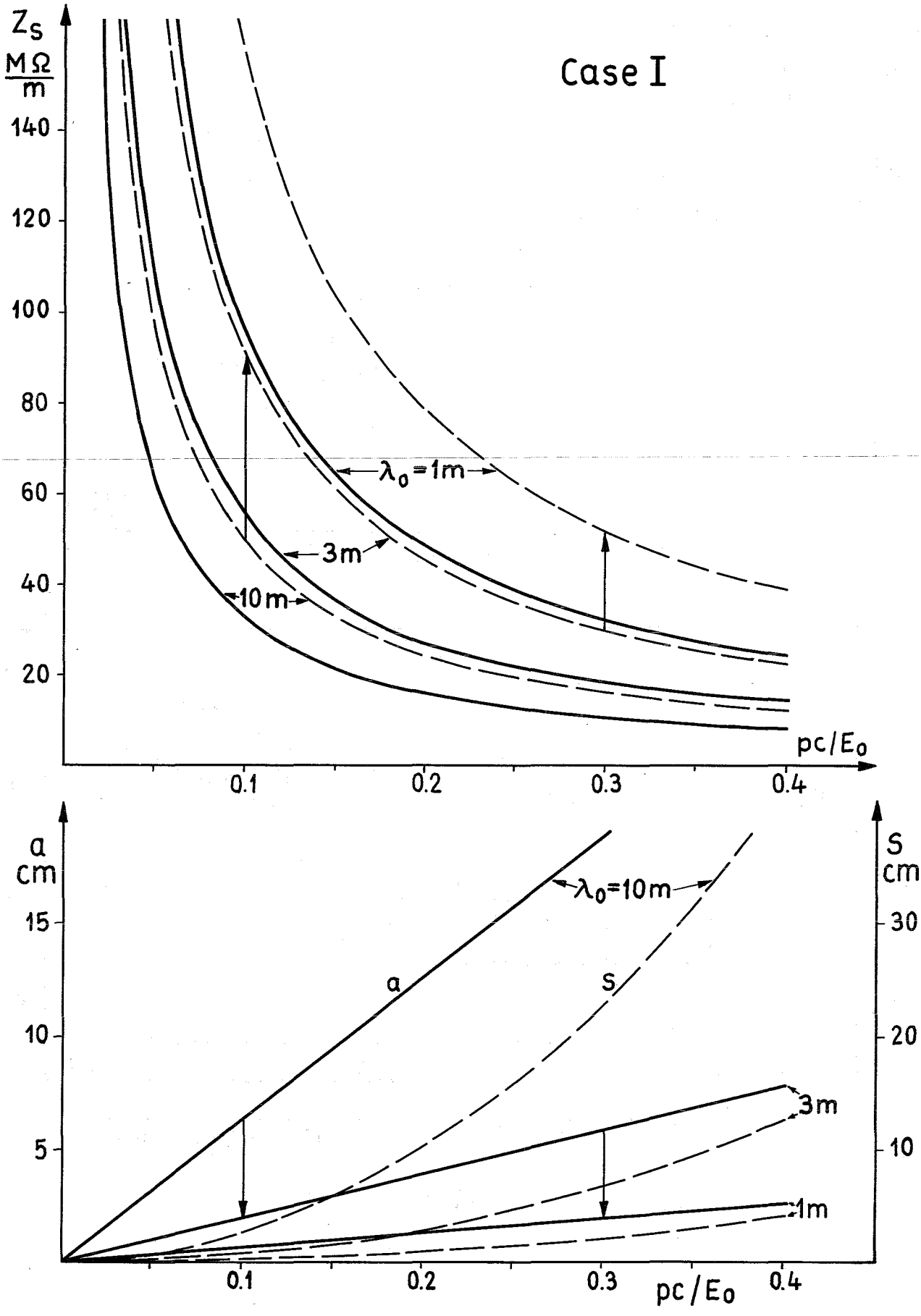
Case I
Z_s
MΩ/m
140
120
100
80
60
40
20
λ_0=1m
3m
10m
pc/E_0
0.1
0.2
0.3
0.4
a
cm
S
cm
15
10
5
30
20
10
λ_0=10m
a
s
3m
1m
0.1
0.2
0.3
pc/E_0
0.4

Fig. 3

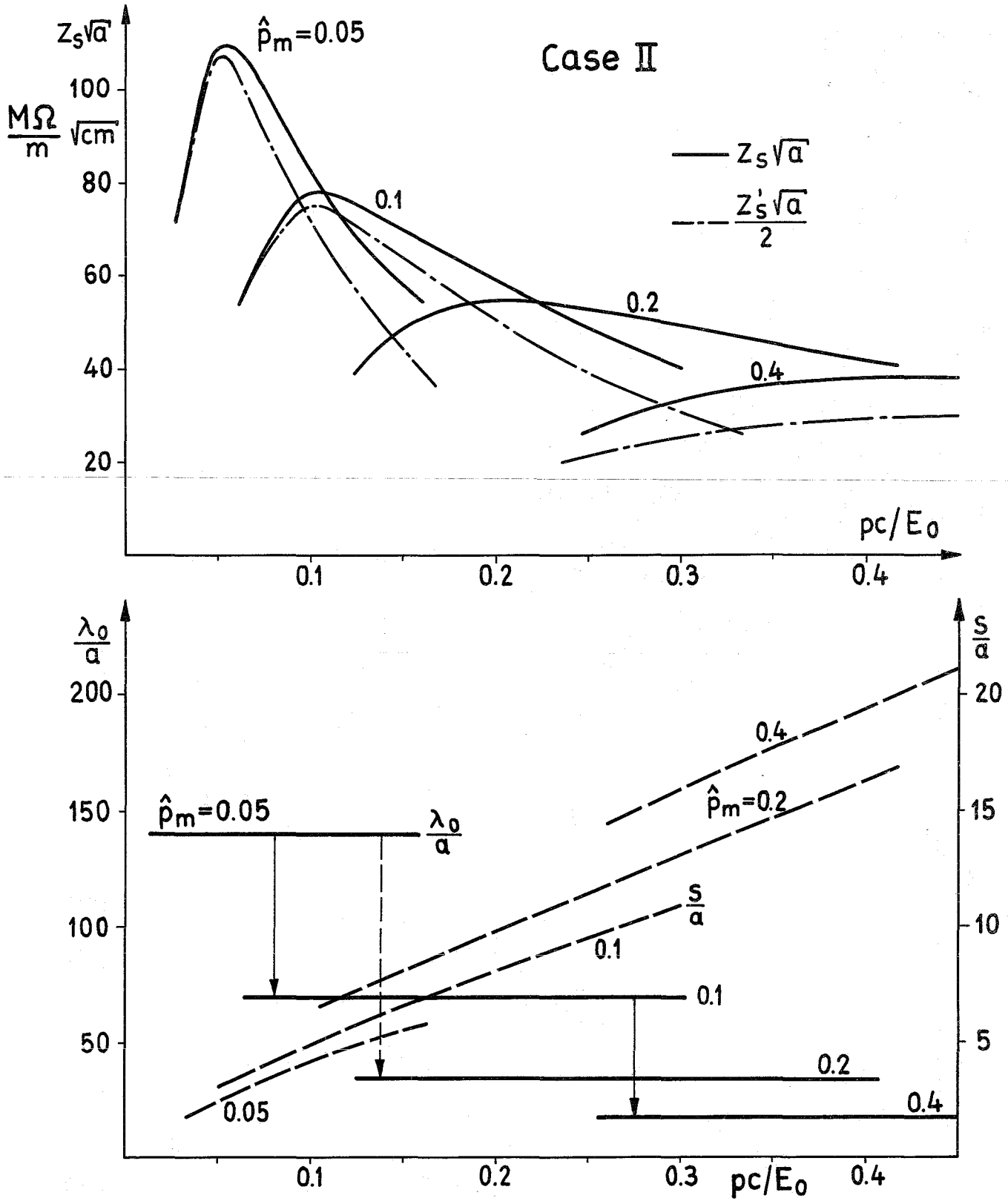
Case II
$Z_s\sqrt{a}$
$\frac{M\Omega}{m}\sqrt{cm}$
$\hat{p}_m=0.05$
0.1
0.2
0.4
$Z_s\sqrt{a}$
$\frac{Z_s'\sqrt{a}}{2}$
100
80
60
40
20
pc/E_0
0.1
0.2
0.3
0.4
$\frac{\lambda_0}{a}$
$\frac{S}{a}$
200
150
100
50
20
15
10
5
$\hat{p}_m=0.05$
$\hat{p}_m=0.2$
0.05
0.1
0.2
0.4

Fig. 4

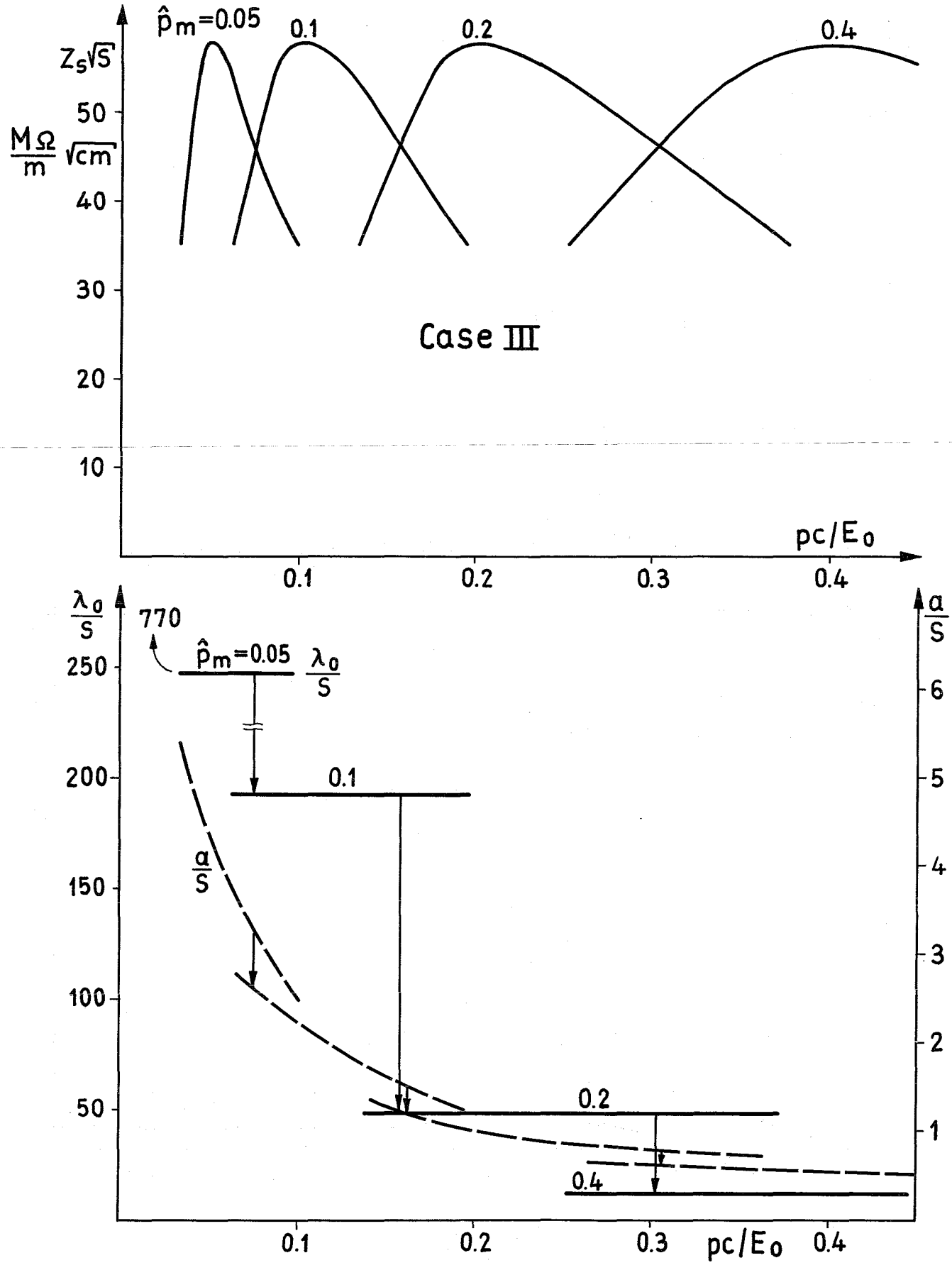
$\hat{p}_m$=0.05
0.1
0.2
0.4
$Z_s\sqrt{S}$
$\frac{M\Omega}{m}\sqrt{cm}$
50
40
30
20
10
Case III
pc/E₀
0.1
0.2
0.3
0.4
$\frac{\lambda_0}{S}$
770
$\hat{p}_m$=0.05
$\frac{\lambda_0}{S}$
250
200
150
100
50
0.1
$\frac{a}{S}$
0.2
0.4
$\frac{a}{S}$
6
5
4
3
2
1
0.1
0.2
0.3
pc/E₀
0.4

Fig. 5

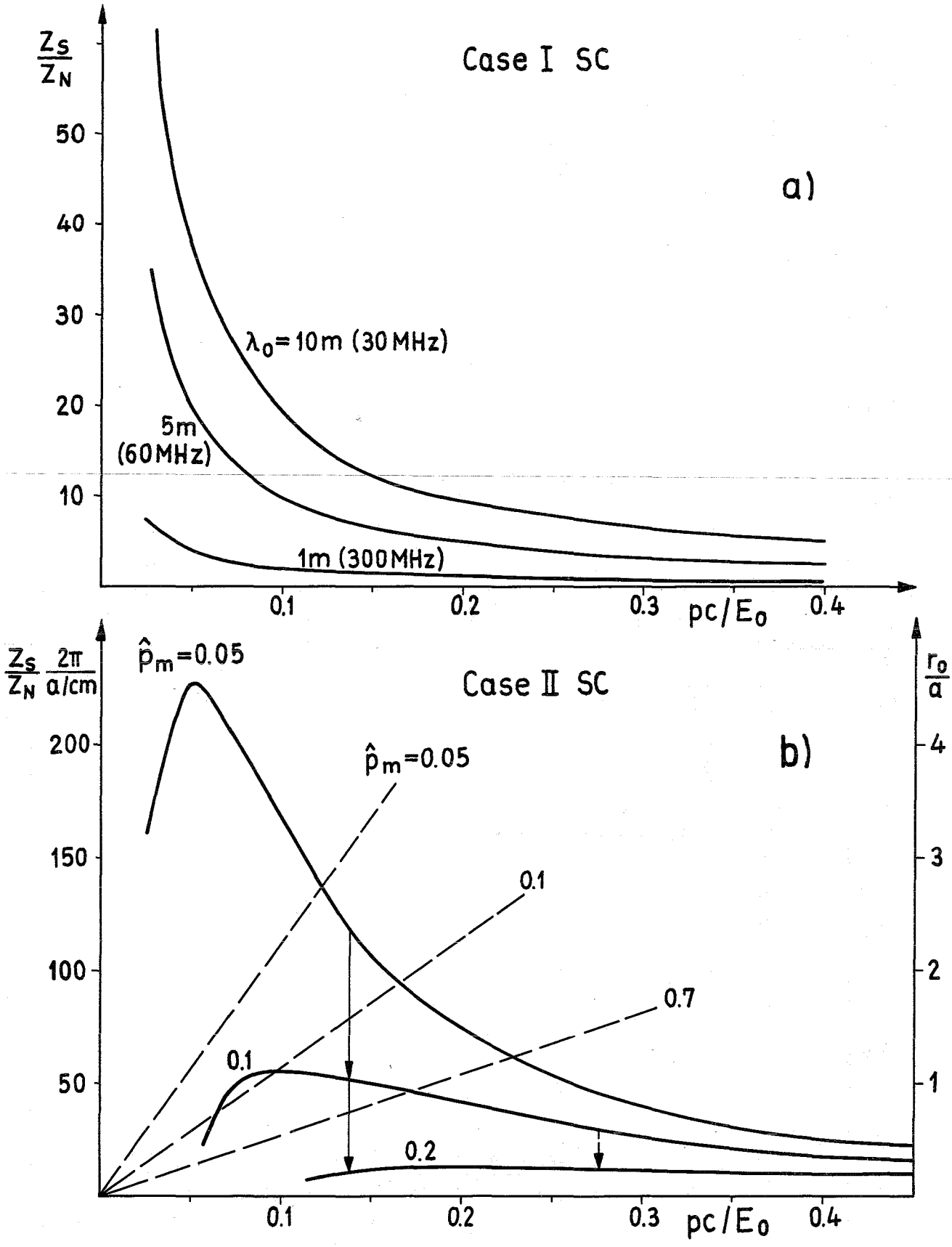
Case I SC
a)
$\frac{Z_S}{Z_N}$
50
40
30
20
10
λ_0= 10m (30 MHz)
5m
(60MHz)
1m (300MHz)
0.1
0.2
0.3
pc/E$_0$
0.4
Case II SC
b)
$\hat{\rho}_m$=0.05
$\frac{Z_S}{Z_N}\frac{2\pi}{a/cm}$
$\frac{r_0}{a}$
200
150
100
50
4
3
2
1
0.1
0.7
0.2

Fig. 6

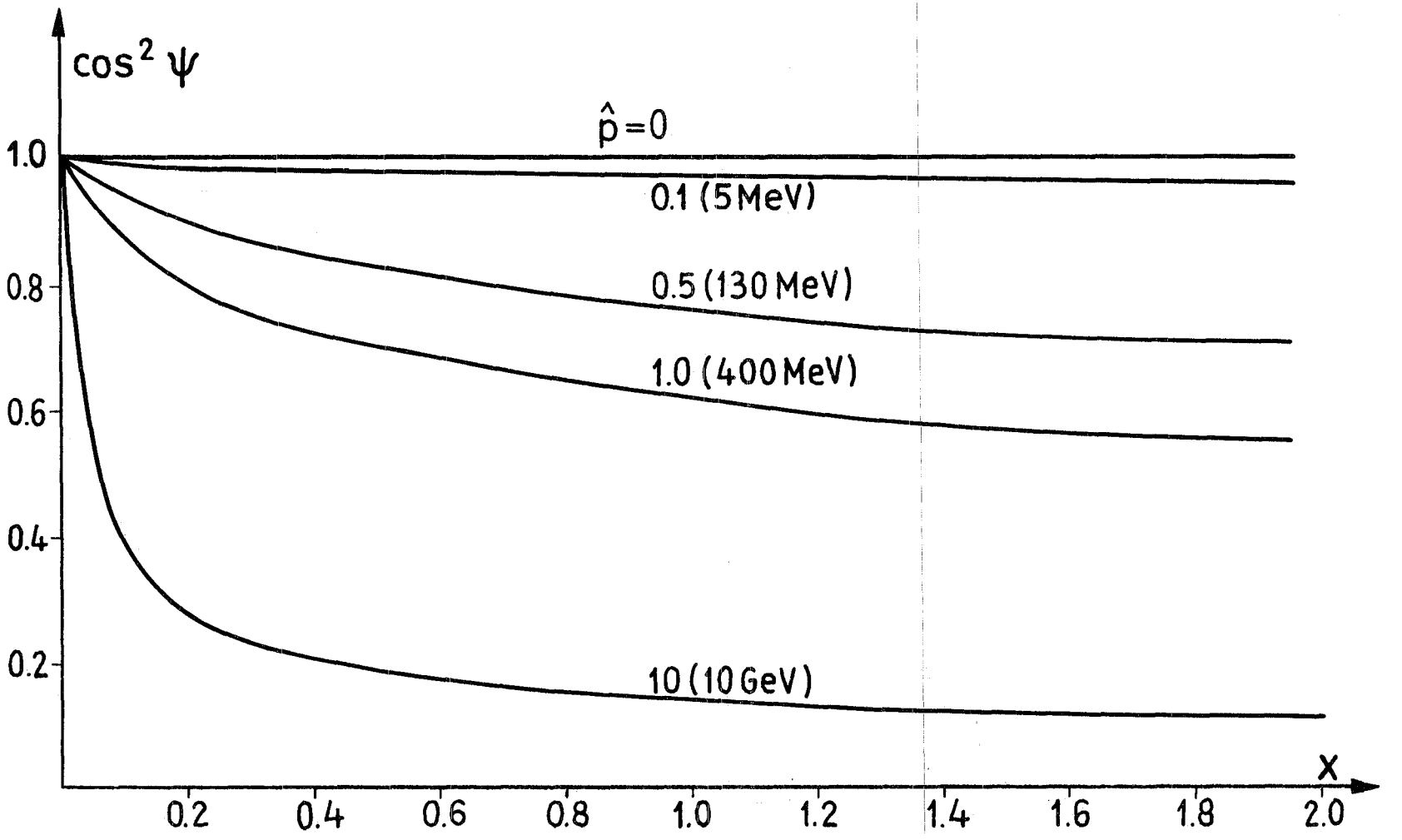
cos² ψ
p̂=0
0.1 (5 MeV)
0.5 (130 MeV)
1.0 (400 MeV)
10 (10 GeV)
1.0
0.8
0.6
0.4
0.2
0.2
0.4
0.6
0.8
1.0
1.2
1.4
1.6
1.8
2.0
X

Fig. 7